

Surgery-induced cryptorchidism induces apoptosis and autophagy of spermatogenic cells in mice

Yi Zheng[†], Pengfei Zhang[†], Conghui Zhang[†] and Wenxian Zeng

College of Animal Science and Technology, Northwest A&F University, Yangling, Shaanxi 712100, China

Research Article

[†]These authors contributed equally to this work.

Cite this article: Yi Zheng *et al.* (2019) Surgery-induced cryptorchidism induces apoptosis and autophagy of spermatogenic cells in mice. *Zygote* 27: 101–110. doi: 10.1017/S096719941900011X

Received: 23 September 18
Revised: 11 January 19
Accepted: 6 February 19
First published online: 19 March 2019

Keywords:

Apoptosis; Autophagy; Cryptorchidism; Spermatogenesis; Testis.

Address for correspondence:

Wenxian Zeng, College of Animal Science and Technology, Northwest A&F University, Yangling, Shaanxi 712100, China.
E-mail: zengwenxian2015@126.com

Summary

Cryptorchidism, characterized by the presence of one (unilateral) or both (bilateral) undescended testes, is a common male urogenital defect. Cryptorchidism can lead to male infertility, testicular cancer being the most extreme clinical symptom, as well as psychological issues of the inflicted individual. Despite this, both knowledge about the aetiology of cryptorchidism and the mechanism for cryptorchidism-induced male infertility remain limited. In this present study, by using an artificial cryptorchid mouse model, we investigated the effects of surgery-induced cryptorchidism on spermatogenic cells and seminiferous epithelial cycles. We found that surgery-induced cryptorchidism led to a reduced testicular weight, aberrant seminiferous epithelial cycles and impaired spermatogenesis characterized by degenerating spermatogenic cells. We also observed multinucleated giant cells after surgery-induced cryptorchidism. Transmission electron microscopy, terminal deoxynucleotidyl transferase dUTP nick end labelling (TUNEL) and western blot assays demonstrated cryptorchidism-induced apoptosis of spermatogenic cells. Moreover, we identified the occurrence of autophagy in germ cells after surgery-induced cryptorchidism. Interestingly, apoptosis and autophagy were synchronous, suggestive of their synergetic roles in promoting germ cell death. Our results provide novel insights into the cryptorchidism-induced male infertility, thereby contributing to the development of male contraceptive strategies as well as treatment options for male infertility caused by cryptorchidism.

Introduction

Approximately one in eight couples suffer from subfertility (Sharlip *et al.*, 2002; Kumar and Singh, 2015), defined as the failure to conceive in the fertile phase of the menstrual cycles after 1 year of unprotected intercourse (Evers, 2002; Gnoth *et al.*, 2005). About half of the cases can be ascribed to male factors (de Kretser, 1997; Evers, 2002). Cryptorchidism, a urogenital birth defect, is a common male factor likely to contribute to subfertility (Lee *et al.*, 1993). Cryptorchidism is characterized by the absence of one (unilateral) or two (bilateral) testes in the scrotum, i.e. without the testis descending from the abdominal cavity to the scrotum through the inguinal canal. It has been known that the temperature in the scrotum is usually 2–8°C lower than that in the abdominal cavity (Ivell, 2007), and is crucial to spermatogenesis. Indeed, previous studies have shown that raised temperature by surgical induction of cryptorchidism impairs spermatogenesis, devastates spermatogenic cells and facilitates the generation of multinucleated giant cells, further expediting the process of germ cell removal (Clegg, 1963; Liu *et al.*, 2012). Nevertheless, the underlying mechanism for this type of germ cell death has been poorly studied.

Cryptorchidism has been reported to induce germ cell apoptosis in mice (Ogi *et al.*, 1998) and rats (Henriksen *et al.*, 1995). Kocak and colleagues (Kocak *et al.*, 2002) considered apoptosis rather than atrophy or necrosis as a principal reason for germ cell death in the cryptorchid testis. Apoptosis, also called type I programmed cell death (PCD), is an energy-dependent active biological process of cellular decomposition characterized by pronounced morphological transformations. Apoptosis can alternatively depend on caspase, and caspase-dependent apoptosis is mainly triggered by the intrinsic mitochondrial pathway and the extrinsic death-receptor pathway (Elmore, 2007; Peterson *et al.*, 2015; Xu *et al.*, 2016). Previous studies have demonstrated that the intrinsic mitochondrial pathway (Absalan *et al.*, 2010; Jung *et al.*, 2015), the Fas system (Ogi *et al.*, 1998) and the p53 signalling pathway (Yin *et al.*, 1998; Absalan *et al.*, 2010) are involved in germ cell apoptosis in the cryptorchid testis. Yet, it remains indefinite whether both intrinsic and extrinsic apoptotic pathways are implicated in this process. In addition, it is unclear when cell apoptosis is initiated and which types of spermatogenic cells undergo apoptosis in the cryptorchid testis.

Unlike apoptosis, autophagy is an evolutionarily conserved intracellular catabolic process. By forming a peculiar double-membrane structure called autophagosome, a portion of the cytoplasm and organelles are engulfed and delivered to the lysosome for degradation (Nakatogawa *et al.*, 2009; Liu *et al.*, 2014; Ohsumi, 2014; Klionsky *et al.*, 2016). Autophagy can consistently occur in all cells at a basal level and increase under various stress conditions such as the presence of intracellular pathogens or inflammation (Deretic, 2006; Chen and Klionsky, 2011), oxidative stress (Coto-Montes *et al.*, 2012), growth factor withdrawn (Song *et al.*, 2012) or heat stress (Zhang *et al.*, 2012). The induction of autophagy and subsequent germ cell death by heat stress suggests that autophagy may also occur in germ cells of the cryptorchid testis that, however, has not been probed before.

In this present study, by using an artificial cryptorchid mouse model, we aimed to increase knowledge about the mechanisms for cryptorchidism-induced male infertility. To be more specific, we aimed to answer the following questions: (1) What are the exact effects of cryptorchidism on spermatogenic cells and seminiferous epithelial cycles? (2) Are apoptosis and autophagy both involved in germ cell death in the cryptorchid testis? (3) If so, what is their crosstalk?

Materials and methods

Animals

Adult (aged 8–9 weeks) Kunming male mice, weighing 34 ± 2 g were obtained from the Fourth Military Medical University (Xi'an, China). All mice were used and maintained under a controlled environment of $25 \pm 5^\circ\text{C}$, 12 h/12 h light/dark cycles, and 30–70% humidity, with food and water *ad libitum*.

Unilateral surgery-induced cryptorchidism

Surgery was performed under avertin (Sigma-Aldrich, 20 $\mu\text{l/g}$) anaesthesia. A midline abdominal incision was made, and the right testis was pulled into the abdominal cavity and sutured to the abdominal wall, while the left testis was maintained in the scrotum. The right testis of control mice was subjected to a sham surgery.

Testicular tissue collection and treatment

Overall, 72 mice were used for three independent experiments ($n=3$). Specifically, in each independent experiment, 21 mice were subjected to surgery-induced cryptorchidism, whereas three mice subjected to a sham surgery were used as controls. The surgery-induced cryptorchid mice were sacrificed on 0.5 day, 1 day, 2 days, 3 days, 4 days, 5 days and 7 days after cryptorchid treatment (three mice for each time point), respectively. Testicular tissue was collected, and then fixed in Bouin's solution (for histological analysis) or 2.5% glutaraldehyde (for ultrastructural analysis). A portion of testicular tissue was frozen in liquid nitrogen (for western blot analysis).

Histological analysis

Testicular tissue from control and surgery-induced cryptorchid mice was fixed in Bouin's solution and embedded in paraffin. Testis sections were sliced at a thickness of 7 μm , deparaffinized and rehydrated. Testis sections were stained with haematoxylin and eosin (HE). After dehydration and embedding, sections were visualized under a Nikon i90 microscope (Nikon, Tokyo, Japan).

Transmission electron microscopy

For ultrastructural analysis, testicular tissue from control and surgery-induced cryptorchid mice was perfused with 2.5% glutaraldehyde. Later, testicular tissue was washed with phosphate-buffered saline (PBS), fixed in 1% OsO_4 for 2 h at 4°C , and embedded in Araldite. Semi-thin sections were stained with toluidine blue and visualized under a light microscope. Ultrathin sections were stained with uranyl acetate and lead citrate, and visualized under a transmission electron microscope (JEM.1010, JEOL, Tokyo, Japan).

TUNEL assay

Terminal deoxynucleotidyl transferase dUTP nick end labelling (TUNEL) assay was performed using a colorimetric TUNEL apoptosis assay kit (Beyotime Institute of Biotechnology, Jiangsu, China), following the manufacturer's instructions. In brief, testis sections were deparaffinized and rehydrated, and then incubated with 20 $\mu\text{g/ml}$ proteinase K (Tiangen, Beijing, China) at room temperature (RT) for 15 min, followed by blocking with 3% H_2O_2 at RT for 10 min to deactivate endogenous peroxidase. The sections were incubated with the TUNEL reaction mix (2 μl terminal deoxynucleotidyl transferase and 48 μl biotin-dUTP) at 37°C for 1 h. The negative TUNEL control was prepared by omitting the enzyme. After washing, the sections were incubated with horseradish peroxidase-conjugated streptavidin solution at RT for 30 min, followed by staining with diaminobenzidine (DAB) and counterstaining with haematoxylin. The slides were later dehydrated and mounted, and visualized under a Nikon i90 microscope (Nikon, Tokyo, Japan).

Western blot

Testicular tissue was ground with liquid nitrogen in a porcelain mortar and lysed in RIPA buffer supplemented with PMSF (Beyotime, Jiangsu, China). Denatured protein samples were electrophoresed on a 12% sodium dodecyl sulfate (SDS) polyacrylamide gel, then transferred to a polyvinylidene fluoride (PVDF) membrane (Millipore, Billerica, USA). The membrane was blocked with 5% non-fat dried milk in Tris-buffered saline with 0.05% Tween-20 (TBST) for 2 h, and then incubated at 4°C overnight with the following primary antibodies: rabbit anti-Bcl-2 (Abcam, 1:1000), rabbit anti-Bax (Cell Signaling Technology, 1:1000), rabbit anti-caspase 8 (Cell Signaling Technology, 1:1000), rabbit anti-caspase 3 (Cell Signaling Technology, 1:1000), rabbit anti-PARP-1 (Cell Signaling Technology, 1:1000), rabbit anti-LC3B (Abcam, 1:1000) and mouse anti- β -actin (Comwin, 1:1000). After washing the next day, the membrane was incubated with horseradish peroxidase-conjugated anti-rabbit or anti-mouse secondary antibody (Abcam, Cambridge, UK, 1:5000) at RT for 2 h. The protein bands were visualized with a Bio-Rad Chemidoc XRS and a Western Bright ECL Kit (Comwin, Beijing, China).

Statistics

Statistical analyses were conducted using SPSS v17.0 software (SPSS, USA). Multiple comparisons were performed using one-way analysis of variance (ANOVA) followed by a least significant difference (LSD) test. Data were presented as the mean \pm standard error of the mean (SEM). A P -value <0.05 was considered to be statistically significant.

Results

Surgery-induced cryptorchidism leads to a reduced testicular weight

We first administered unilateral cryptorchid treatment on adult mice. In brief, the right testis was pulled into the abdominal cavity and sutured to the abdominal wall, while the left testis was maintained in the scrotum. The right testis of mice subjected to a sham surgery was used as a control. The testicular weight experienced a steady decrease from day 4 after cryptorchid treatment and reached the bottom on day 7 (Fig. 1).

Surgery-induced cryptorchidism leads to aberrant seminiferous epithelial cycles and impaired spermatogenesis

Next, we performed histological analysis on testis sections from control and surgery-induced cryptorchid mice. Compared with the control, there was no significant morphological difference on day 0.5 after surgery-induced cryptorchid treatment. Nevertheless, aberrant seminiferous epithelial cycles and impaired spermatogenesis were observed later. On day 1, some pachytene spermatocytes at stages VII–VIII (Fig. 2e) and I–IV (Fig. 2g), as well as some dividing spermatocytes at stage XII (Fig. 2f) showed pyknotic nuclei. Round spermatids at stages VII–VIII (Fig. 2e) and I–IV (Fig. 2g) disappeared from the seminiferous epithelium. On day 3, some pachytene spermatocytes at stages V–VI and IX–X showed pyknotic nuclei. Some round spermatids at the stage VIII (Fig. 2i) displayed typical ring-like nuclei. At stages V–VI and IX–X, spermatids were absent in the seminiferous epithelium. On day 5, seminiferous tubules with rare or no round spermatids were discerned, and pachytene and onward spermatocytes disappeared from the seminiferous epithelium. On day 7, most spermatocytes degenerated and showed pyknotic (Fig. 2q) or even ring-like nuclei (Fig. 2r, t, left arrows). At this time point, it was difficult to recognize some seminiferous epithelial cycles. Moreover, we observed multinucleated giant cells (Fig. 2r–t, right arrows) in almost all seminiferous tubules of the cryptorchid testis. These multinucleated giant cells contained aggregates of degenerating spermatocytes and round spermatids.

Surgery-induced cryptorchidism induces apoptosis of spermatogenic cells

To demonstrate the occurrence of cell apoptosis in the cryptorchid testis, we first performed a transmission electron microscopy study. We observed that apoptosis was initiated on day 3 after cryptorchid treatment, characterized by the formation of pyknotic chromatin and concrete nucleoli (Fig. 3g–i, arrows). On day 7, concentrated organelles (Fig. 3j, arrow) were observed. Moreover, apoptotic

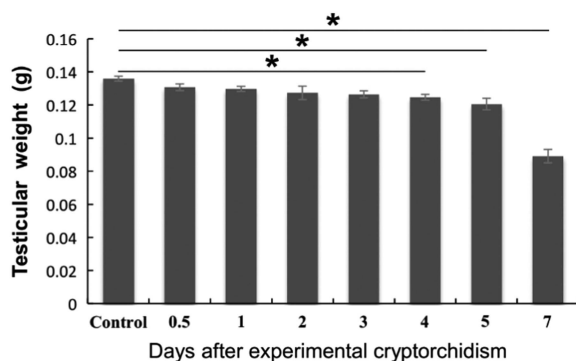


Figure 1. Effects of surgery-induced cryptorchidism on the testicular weight. Data are presented as the mean \pm standard error of the mean (SEM), $n = 3$. * $P < 0.05$.

bodies (Fig. 3k, arrows), which contain cellular components such as organelles and fragments of nuclear chromatin, became discernible, indicative of progressive cell apoptosis.

Next, we performed a TUNEL assay on testis sections from control and surgery-induced cryptorchid mice. We observed that the majority of TUNEL⁺ apoptotic cells occurred at day 4 after treatment (Fig. 4g–i, arrows). TUNEL⁺ apoptotic cells mainly consisted of pachytene spermatocytes, a few round spermatids and rare spermatogonia. Some multinucleated giant cells were also positive for TUNEL signalling (Fig. 4i, arrow). To assess germ cell apoptosis in the cryptorchid testis, we quantified the percentage of seminiferous tubules harbouring TUNEL⁺ cells (Fig. 4j), the average number of total TUNEL⁺ cells (Fig. 4k) and TUNEL⁺ multinucleated giant cells (Fig. 4l) per seminiferous tubule, as well as the percentage of TUNEL⁺ multinucleated giant cells in all TUNEL⁺ cells (Fig. 4m). Compared with the control, the percentage of seminiferous tubules harbouring TUNEL⁺ cells (Fig. 4j) and the number of total TUNEL⁺ cells (Fig. 4k) gradually increased from day 4 after cryptorchid treatment and reached the peak on day 7. Surgery-induced cryptorchidism also facilitated the formation of TUNEL⁺ multinucleated giant cells (Fig. 4l, m).

Next, we performed a western blot assay to detect the expression of apoptosis-related proteins in the control and cryptorchid mouse testis. Bcl-2 (the anti-apoptosis protein) and Bax (the pro-apoptosis protein) are two important members of the Bcl-2 family regulating the intrinsic mitochondrial apoptotic pathway (Kaur and Bansal, 2015). Consistently, the expression of Bcl-2 gradually decreased (Fig. 5a,b), whereas that of Bax showed an upward trend after day 1 after surgery-induced cryptorchid treatment (Fig. 5a,c). Previous reports have shown that caspase-8 and caspase-3 are cleaved and activated in the extrinsic death-receptor apoptotic pathway (Fan *et al.*, 2013). In our present study, with time, surgery-induced cryptorchidism caused the increasing cleaved caspase-8 (Fig. 5a, d), caspase-3 (Fig. 5a, e) as well as PARP-1 (Fig. 5a, f). These overall results suggest that both intrinsic and extrinsic pathways are involved in the germ cell apoptosis of cryptorchid mice.

Surgery-induced cryptorchidism induces autophagy of spermatogenic cells

Finally, we investigated whether autophagy occurs in germ cells of the cryptorchid mouse testis. Autophagy can be characterized by the formation of double-membrane structures called autophagosome (Kliosnyk *et al.*, 2016). To this end, we performed an additional transmission electron microscopy study, and observed typical autophagosome in germ cells from day 3 after cryptorchid treatment (Fig. 6a–f).

LC3 is a mammalian homologue of the yeast Apg8p protein. There are two forms of LC3 (LC3-I and LC3-II), and the conversion of LC3-I to LC3-II serves as a marker for autophagy (Kabeya *et al.*, 2000). Therefore we performed a western blot assay to detect the expression of LC3-I and LC3-II in the control and cryptorchid mouse testis. Indeed, the ratio of LC3-II/LC3-I increased with time and reached a peak on day 7 after cryptorchid treatment (Fig. 6g, h). Collectively, the results indicated that surgery-induced cryptorchidism induces autophagy of spermatogenic cells.

Discussion

Cryptorchidism, characterized by the presence of one (unilateral) or both (bilateral) undescended testes, is a common male

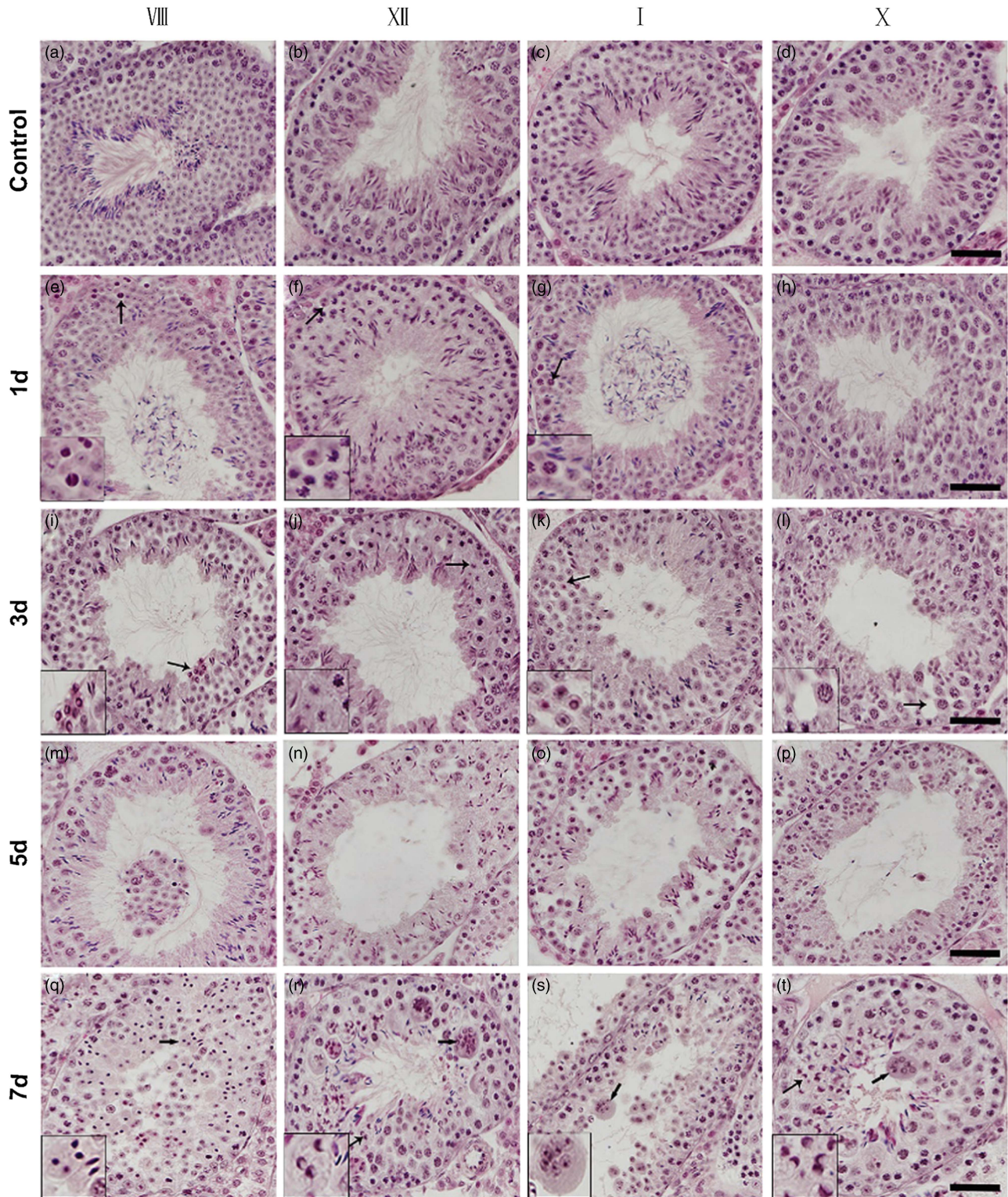


Figure 2. Histological analysis of testis sections from control and surgery-induced cryptorchid mice. (a–d) Representative images of testis sections from control mice showing normal spermatogenesis. (e–t) Representative images of testis sections on day 1 (e–h), day 3 (i–l), day 5 (m–p) and day 7 (q–t) after surgery-induced cryptorchid treatment. Insets are the magnification of indicated areas. Bar represents 100 μm .

urogenital defect. Cryptorchidism can lead to male infertility (Lee *et al.*, 1993), testicular cancer being the most extreme clinical symptom (Pettersson *et al.*, 2007), as well as psychological issues of the inflicted individual (Xi *et al.*, 2015). Despite this, knowledge about the aetiology of cryptorchidism and the mechanism for

cryptorchidism-induced male infertility remain limited. Here, we took advantage of an artificial cryptorchid mouse model to systematically investigate the effect of surgery-induced cryptorchidism on spermatogenic cells and seminiferous epithelial cycles. We found that surgery-induced cryptorchidism led to a reduced

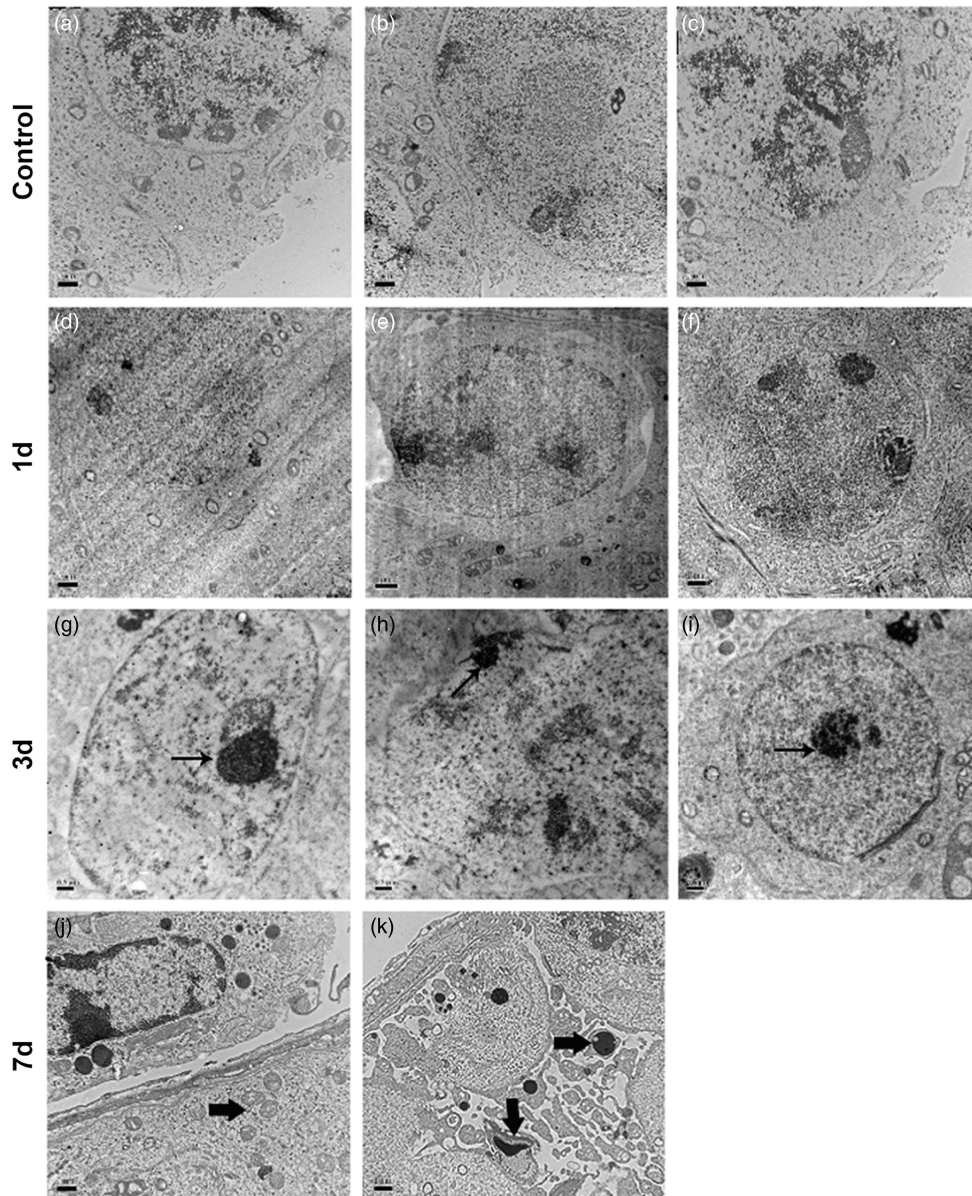


Figure 3. Representative transmission electron micrographs of testis sections from control and surgery-induced cryptorchid mice. (a–f) Representative micrographs of testis sections from control (a–c) and cryptorchid mice 1 day after treatment (d–f) showing normal cell morphology. (g–k) Representative micrographs of testis sections on day 3 (g–i) and day 7 (j, k) after surgery-induced cryptorchid treatment. Bar represents 1 μ m.

testicular weight, aberrant seminiferous epithelial cycles and impaired spermatogenesis characterized by degenerating spermatogenic cells. Moreover, we identified that both apoptosis and autophagy were involved in germ cell death of the cryptorchid testis. Overall, our results provide novel insights into the cryptorchidism-induced male infertility, thereby contributing to the development of male contraceptive strategies and, more importantly, treatment options for male infertility caused by cryptorchidism.

Spermatogenesis is a highly efficient, intricate and precise process in testes by which lifelong male fertility is maintained. Crucial to this process is the appropriate temperature in the scrotum, which is usually 2–8°C lower than that in the abdominal cavity (Ivell, 2007). Indeed, higher temperatures often leads to disrupted spermatogenesis (Schulz and Miura, 2002). In our study, testicular weight experienced a sharp decrease from day 4

after surgery-induced cryptorchid treatment, in accordance with a previous report (Yin *et al.*, 1997) and a study that involved intra-scrotal heat stress in mice (Lin *et al.*, 2015). The underlying reason for the reduced testicular weight is likely to be the death and later large-scale elimination of spermatogenic cells.

Raised temperature by surgical induction of cryptorchidism can impair spermatogenesis, devastate spermatogenic cells and disrupt seminiferous epithelial cycles (Clegg, 1963). In our present study, we observed the initiation of morphological abnormality in pachytene spermatocytes at stages VII–VIII and I–IV, and in dividing spermatocytes at stage XII on day 1 after cryptorchid treatment, in line with a previous report (Henriksen *et al.*, 1995). Chowdhury and Steinberger (1970) reported the initiation of morphological abnormality in pachytene spermatocytes at stages X–XII, in dividing spermatocytes at stages XIII–XIV and in round spermatids at the stage I, and that the morphological alterations

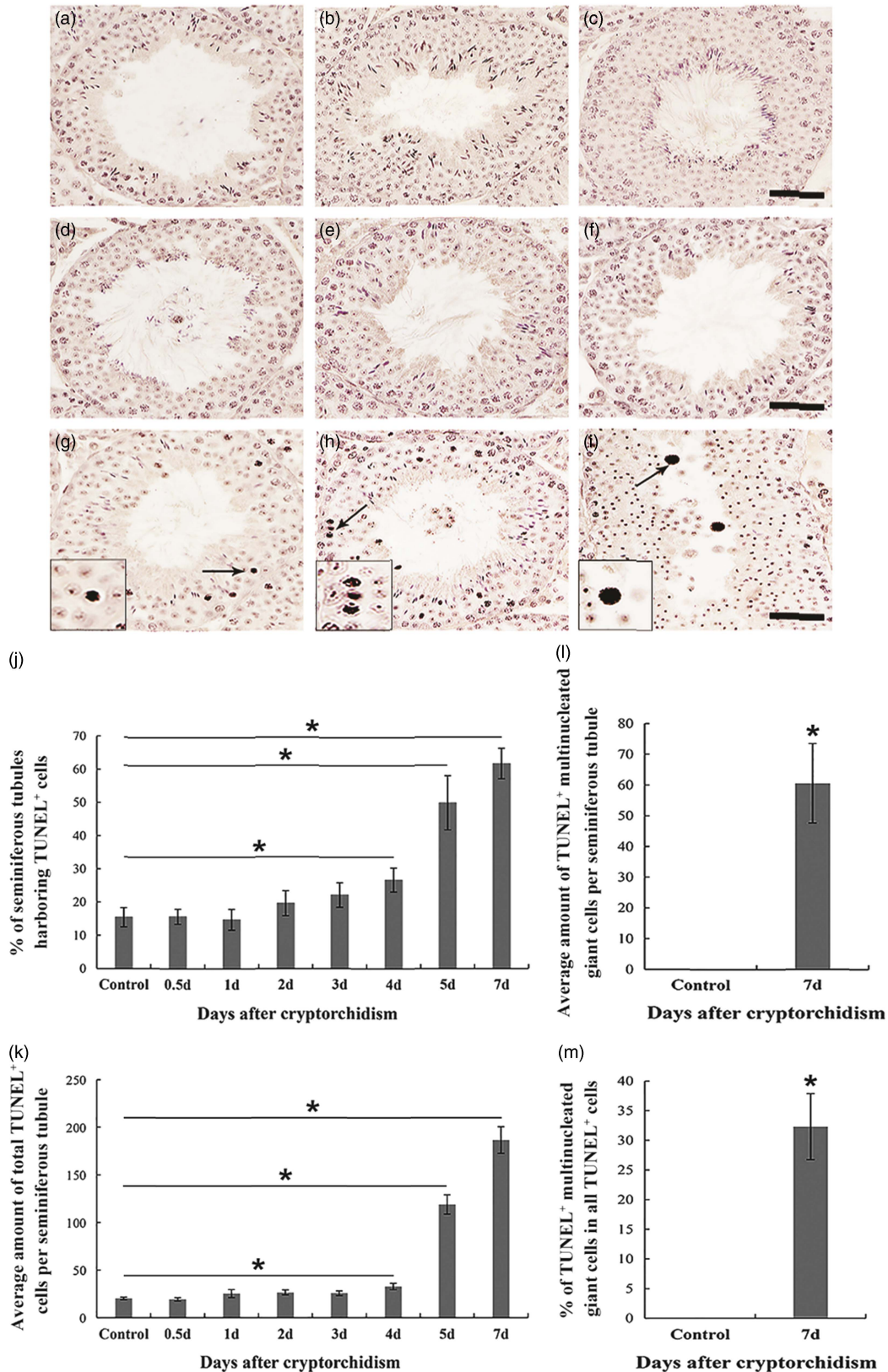


Figure 4. TUNEL assay of testis sections from control and surgery-induced cryptorchid mice. (a) Negative TUNEL control. (b) TUNEL assay of testis sections from control mice. (c–i) TUNEL assay of testis sections on day 0.5 (c), day 1 (d), day 2 (e), day 3 (f), day 4 (g), day 5 (h) and day 7 (i) after surgery-induced cryptorchid treatment. Insets are the magnification of indicated areas. Bar represents 100 μm . (j) Percentages of seminiferous tubules harbouring TUNEL⁺ cells. (k) Average number of total TUNEL⁺ cells per seminiferous tubule. (l) Average number of TUNEL⁺ multinucleated giant cells per seminiferous tubule. (m) Percentages of TUNEL⁺ multinucleated giant cells in all TUNEL⁺ cells. Data are presented as the mean \pm standard error of the mean (SEM), $n = 3$. * $P < 0.05$. In each independent experiment, overall 100 seminiferous tubules were examined.

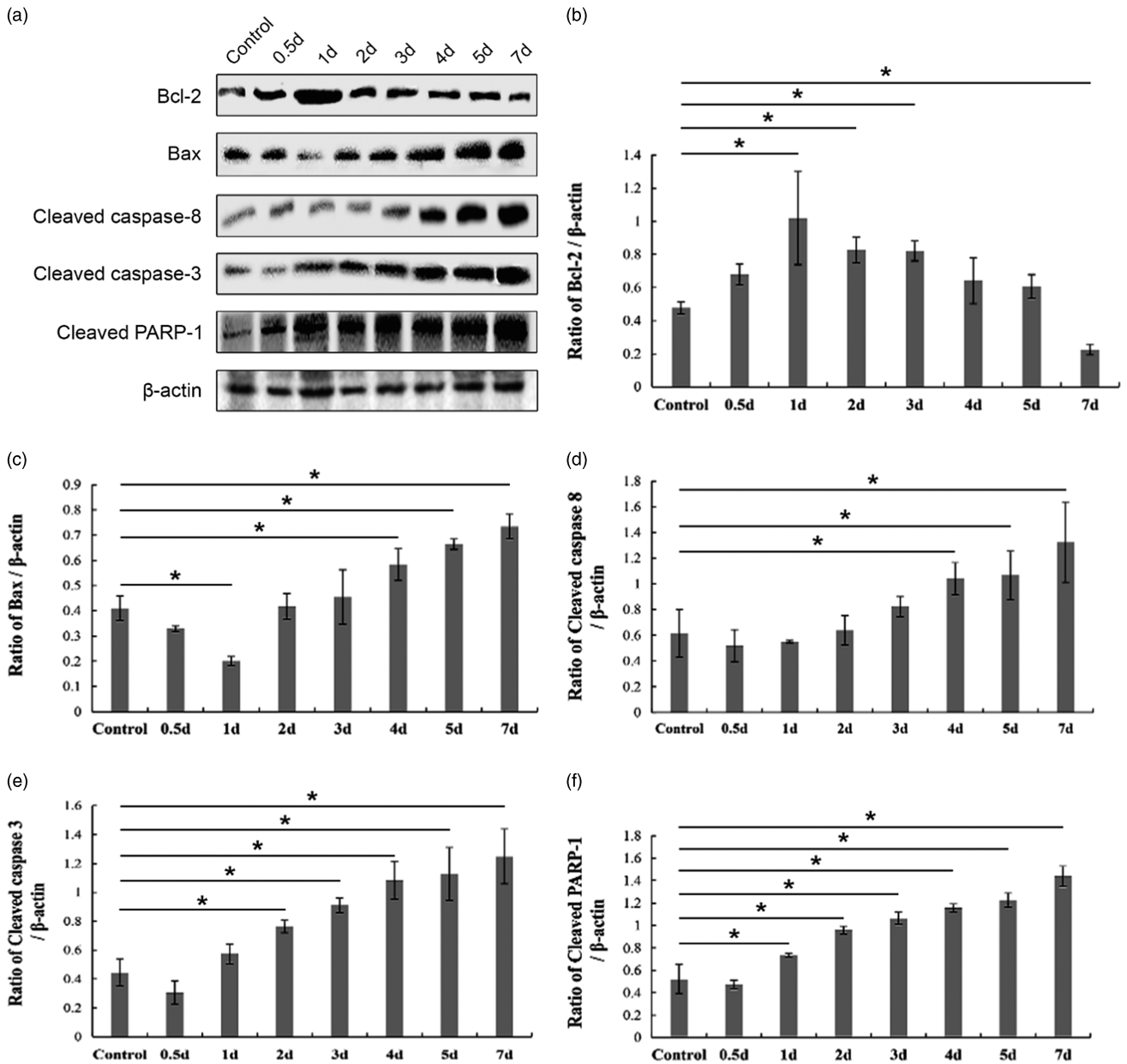


Figure 5. Western blot analysis of apoptosis-related protein levels in the control and surgery-induced cryptorchid mouse testes. (a) Representative images of immunoblotting. β -actin is used as a loading control. The band intensity of Bcl-2 (b), Bax (c), cleaved caspase-8 (d), cleaved caspase-3 (e) and cleaved PARP-1 (f) is divided by that of β -actin, respectively. Data are presented as the mean \pm standard error of the mean (SEM), $n=3$. * $P < 0.05$.

could be observed in as early as 1 hour following exposure of rat testes to 43°C for 15 min. The inconsistent outcome might be ascribed to distinct treatment (surgery-induced cryptorchidism versus intra-scrotal heat stress) and species (mice versus rats).

We observed multinucleated giant cells in seminiferous tubules on day 7 after cryptorchid treatment. Multiple reports have demonstrated the emergence of multinucleated giant cells in cryptorchid testes (Clegg, 1963; Kerr *et al.*, 1979; Yin *et al.*, 1998; Kumar *et al.*, 2012). Multinucleated giant cells are therefore regarded as a marker for the cryptorchid seminiferous epithelium. Nantel and co-workers (Nantel *et al.*, 1996) reported that multinucleated giant cells were associated with cell apoptosis. Indeed, the formation of multinucleated giant cells can be perceived as a response to cryptorchidism, and it is these cells that further expedite the process of germ cell removal. A decline in intra-

testicular testosterone may act as a catalyst for the formation of these cells (Shikone *et al.*, 1994; Barqawi *et al.*, 2004).

In normal rat testes, apoptosis is mainly observed in spermatogonia (Allan *et al.*, 1992). Nonetheless, previous studies have shown that in mice, primary spermatocytes and round spermatids are most vulnerable to heat stress and prone to undergo apoptosis (Lue *et al.*, 1999; Yin *et al.*, 1997; Zhang *et al.*, 2012). In our present study, we found that TUNEL⁺ apoptotic cells were mainly comprised of pachytene spermatocytes, a few round spermatids and rare spermatogonia, indicating that, in surgery-induced cryptorchid mouse testes, pachytene spermatocytes are the predominant cell type undergoing apoptosis. Notably, not all multinucleated giant cells were positive for the TUNEL signalling, suggesting that non-apoptotic multinucleated giant cells may also contribute to germ cell removal in the cryptorchid testis.

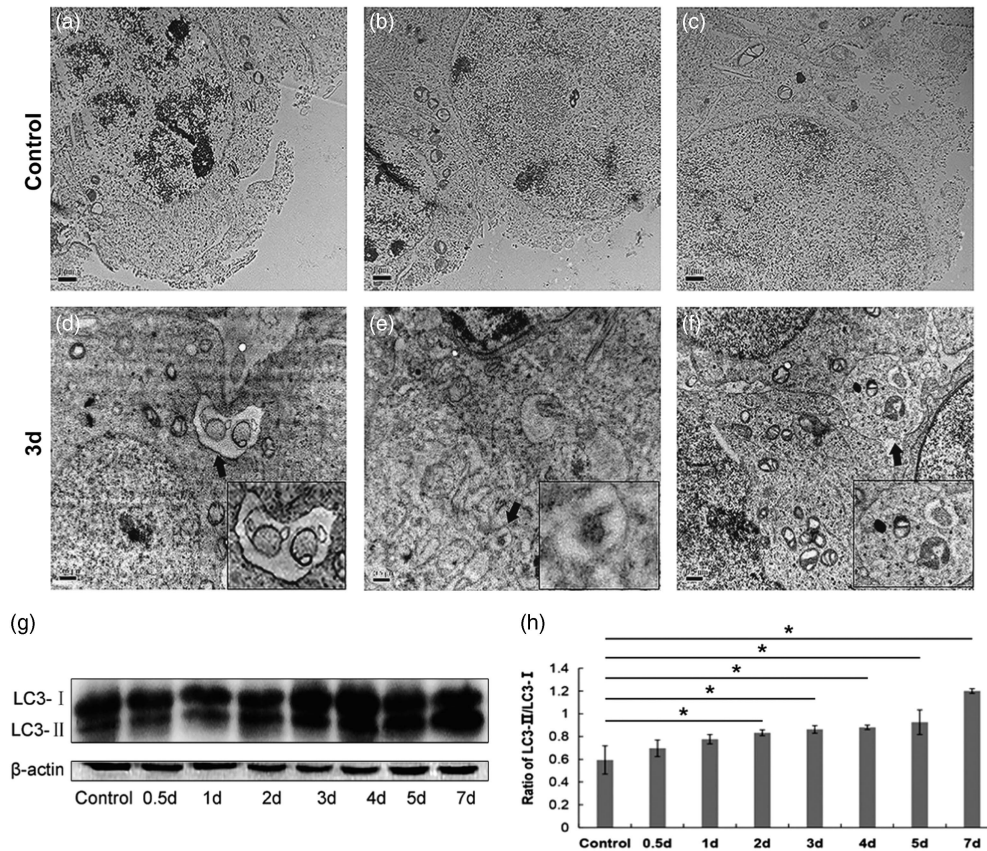


Figure 6. Surgery-induced cryptorchidism induces autophagy of spermatogenic cells. (a–f) Representative transmission electron micrographs of testis sections from control (a–c) and cryptorchid mice on day 3 after cryptorchid treatment (d–f). Arrows show the typical autophagosome. Insets are the magnification of indicated areas. Bar represents 1 μ m. (g) Western blot analysis of LC3-I and LC3-II levels in the control and surgery-induced cryptorchid mouse testis. β -Actin is used as a loading control. (h) The ratio of the band intensity of LC3-II/LC3-I. Data are presented as the mean \pm standard error of the mean (SEM), $n=3$. * $P < 0.05$.

Apoptotic multinucleated giant cells seem to be unique to testes, and the adjacent Sertoli cells may play a role in the formation of these multinucleated giant cells (Yin *et al.*, 1997; Chaki *et al.*, 2005).

Apoptosis mostly depends on caspase, and caspase-dependent apoptosis is mainly triggered by the intrinsic mitochondrial pathway and the extrinsic death-receptor pathway. The intrinsic pathway is mainly regulated by the Bcl-2 protein family (Kaur and Bansal, 2015). Bcl-2, as well as its structural homologue, the long form of Bcl-x (Bcl-x_L), facilitate cell survival by inhibiting apoptosis (Boise *et al.*, 1993; Absalan *et al.*, 2010), while other members of the Bcl-2 protein family, such as Bax, Bak and Bad, promote cell apoptosis (Oltvai *et al.*, 1993; Yang *et al.*, 1995; Kheradmand *et al.*, 2011). In the extrinsic pathway, caspase-8 and caspase-3 are successively cleaved and activated. Yet, regardless of the intrinsic (which involves activation of caspase-9) or extrinsic pathway (which involves activation of caspase-8), the cleavage of the downstream executioner caspase-3 ensues, eventually resulting in apoptosis (Hikim *et al.*, 2003). In our present study, the expression of Bcl-2 gradually decreased, whereas that of Bax, cleaved caspase-8, caspase-3 as well as PARP-1 showed an upward trend from day 1 after surgery-induced cryptorchid treatment, suggesting that both intrinsic and extrinsic pathways are involved in germ cell apoptosis of cryptorchid mice. In addition, by transmission electron microscopy, we observed that apoptosis was initiated on day 3 after cryptorchid treatment, characterized by the formation of pyknotic chromatin and

concrete nucleoli. These results provided new insights for studies on germ cell apoptosis in the cryptorchid testis.

Autophagy can consistently occur in all cells at a basal level and increase under various stress conditions such as the presence of intracellular pathogens or inflammation (Deretic, 2006; Chen and Klionsky, 2011), oxidative stress (Coto-Montes *et al.*, 2012), growth factor withdrawn (Song *et al.*, 2012) or heat stress (Zhang *et al.*, 2012). Here we suggest that, like heat stress, cryptorchidism can induce autophagy of spermatogenic cells. Interestingly, by transmission electron microscopy, we observed typical autophagosome in germ cells from day 3 after cryptorchid treatment, when apoptosis was also initiated. Both apoptosis and autophagy fall within the scope of PCD. Nonetheless, their crosstalk remains elusive in most cell types under variable conditions. First, autophagy can occur prior to apoptosis and then promote apoptosis. Second, autophagy and apoptosis can antagonize each other thereby promoting cell survival/death. Third, autophagy and apoptosis can interconvert to each other under certain conditions, eventually safeguarding cell death (Gozuacik and Kimchi, 2007; Maiuri *et al.*, 2007; Eisenberg-Lerner *et al.*, 2009; Gump and Thorburn, 2011). Our study showed the synchronous and progressive apoptosis and autophagy after cryptorchid treatment, suggestive of their synergetic roles in promoting germ cell death. Future studies on mechanisms regulating apoptosis and autophagy of germ cells in the cryptorchid testis may provide insight for resolving male fertility issues, e.g. sterility and failure to conceive.

Financial support. This study was supported in part by National Key R&D Programme of China (2018YFD0501000), the National Natural Science Foundation of China (Grant No. 31572401) to WZ; Young Talent fund of University Association for Science and Technology in Shaanxi, China (Grant No. 20180204), China Postdoctoral Science Foundation (Grant No. 2018M641032) and a startup fund from Northwest A&F University (Grant No. Z109021803) to YZ.

Conflicts of interest. The authors declare no conflicts of interest.

Ethical standards. All experimental procedures involving mice were approved by the Institutional Animal Care and Use Committee of the Northwest A&F University.

References

- Absalan F, Movahedin M and Mowla SJ** (2010) Germ cell apoptosis induced by experimental cryptorchidism is mediated by molecular pathways in mouse testis. *Andrologia* **42**, 5–12.
- Allan DJ, Harmon BV and Roberts SA** (1992) Spermatogonial apoptosis has three morphologically recognizable phases and shows no circadian rhythm during normal spermatogenesis in the rat. *Cell Proliferat* **25**, 241–50.
- Barqawi A, Trummer H and Meacham R** (2004) Effect of prolonged cryptorchidism on germ cell apoptosis and testicular sperm count. *Asian J Androl* **6**, 47–51.
- Boise LH, Gonzalez-Garcia M, Postema CE, Ding L, Lindsten T, Turka LA, Mao X, Nunez G and Thompson CB** (1993) bcl-x, a bcl-2-related gene that functions as a dominant regulator of apoptotic cell death. *Cell* **74**, 597–608.
- Chaki SP, Misro MM, Ghosh D, Gautam DK and Srinivas M** (2005) Apoptosis and cell removal in the cryptorchid rat testis. *Apoptosis* **10**, 395–405.
- Chen Y and Klionsky DJ** (2011) The regulation of autophagy—unanswered questions. *J Cell Sci* **124**, 161–70.
- Chowdhury AK and Steinberger E** (1970) Early changes in the germinal epithelium of rat testes following exposure to heat. *J Reprod Fertil* **22**, 205–12.
- Clegg EJ** (1963) Studies on artificial cryptorchidism: degenerative and regenerative changes in the germinal epithelium of the rat testis. *J Endocrinol* **27**, 241–51.
- Coto-Montes A, Boga JA, Rosales-Corral S, Fuentes-Broto L, Tan DX and Reiter RJ** (2012) Role of melatonin in the regulation of autophagy and mitophagy: a review. *Mol Cell Endocrinol* **361**, 12–23.
- de Kretser DM** (1997) Male infertility. *Lancet* **349**, 787–90.
- Deretic V** (2006) Autophagy as an immune defense mechanism. *Curr Opin Immunol* **18**, 375–82.
- Eisenberg-Lerner A, Bialik S, Simon HU and Kimchi A** (2009) Life and death partners: apoptosis, autophagy and the cross-talk between them. *Cell Death Differ* **16**, 966–75.
- Elmore S** (2007) Apoptosis: a review of programmed cell death. *Toxicol Pathol* **35**, 495–516.
- Evers JL** (2002) Female subfertility. *Lancet* **360**, 151–9.
- Fan Q, Huang ZM, Boucher M, Shang X, Zuo L, Brinks H, Lau WB, Zhang J, Chuprun JK and Gao E** (2013) Inhibition of Fas-associated death domain-containing protein (FADD) protects against myocardial ischemia/reperfusion injury in a heart failure mouse model. *PLoS One* **8**, e73537.
- Gnoth C, Godehardt E, Frank-Herrmann P, Friol K, Tigges J and Freundl G** (2005) Definition and prevalence of subfertility and infertility. *Hum Reprod* **20**, 1144–7.
- Gozaacik D and Kimchi A** (2007) Autophagy and cell death. *Curr Topics Dev Biol* **78**, 217–45.
- Gump JM and Thorburn A** (2011) Autophagy and apoptosis: what is the connection? *Trends Cell Biol* **21**, 387–92.
- Henriksen K, Hakovirta H and Parvinen M** (1995) In-situ quantification of stage-specific apoptosis in the rat seminiferous epithelium: effects of short-term experimental cryptorchidism. *Int J Androl* **18**, 256–62.
- Hikim AP, Lue Y, Yamamoto CM, Vera Y, Rodriguez S, Yen PH, Soeng K, Wang C and Swerdloff RS** (2003) Key apoptotic pathways for heat-induced programmed germ cell death in the testis. *Endocrinology* **144**, 3167–75.
- Ivell R** (2007) Lifestyle effect and the biology of the human scrotum. *Reprod Biol Endocrinol* **5**, 15.
- Jung KY, Yon JM, Lin C, Jung AY, Lee JG, Baek IJ, Lee BJ, Yun YW and Nam SY** (2015) Phospholipid hydroperoxide glutathione peroxidase is involved in the maintenance of male fertility under cryptorchidism in mice. *Reprod Toxicol* **57**, 73–80.
- Kabeya Y, Mizushima N, Ueno T, Yamamoto A, Kirisako T, Noda T, Kominami E, Ohsumi Y and Yoshimori T** (2000) LC3, a mammalian homologue of yeast Apg8p, is localized in autophagosome membranes after processing. *EMBO J* **19**, 5720–8.
- Kaur S and Bansal MP** (2015) Protective role of dietary-supplemented selenium and vitamin E in heat-induced apoptosis and oxidative stress in mice testes. *Andrologia* **47**, 1109–19.
- Kerr JB, Rich KA and de Kretser DM** (1979) Effects of experimental cryptorchidism on the ultrastructure and function of the Sertoli cell and peritubular tissue of the rat testis. *Biol Reprod* **21**, 823–38.
- Kheradmand A, Dezfoulian O and Tarrahi MJ** (2011) Ghrelin attenuates heat-induced degenerative effects in the rat testis. *Regul Pept* **167**, 97–104.
- Kliosnky D et al.** (2016) Guidelines for the use and interpretation of assays for monitoring autophagy 3rd edn. *Autophagy* **12**, 1–222.
- Kocak I, Dundar M, Hekimgil M and Okyay P** (2002) Assessment of germ cell apoptosis in cryptorchid rats. *Asian J Androl* **4**, 183–6.
- Kumar N and Singh AK** (2015) Trends of male factor infertility, an important cause of infertility: a review of the literature. *J Hum Reprod Sci* **8**, 191–6.
- Kumar V, Misro MM and Datta K** (2012) Simultaneous accumulation of hyaluronan binding protein 1 (HABP1/p32/gC1qR) and apoptotic induction of germ cells in cryptorchid testis. *J Androl* **33**, 114–21.
- Lee PA, Bellinger MF, Songer NJ, O'Leary L, Fishbough R and LaPorte R** (1993) An epidemiologic study of paternity after cryptorchidism: initial results. *Eur J Pediatr* **152**(Suppl 2), S25–7.
- Lin C, Shin DG, Park SG, Chu SB, Gwon LW, Lee JG, Yon JM, Baek IJ and Nam SY** (2015) Curcumin dose-dependently improves spermatogenic disorders induced by scrotal heat stress in mice. *Food Function* **6**, 3770–7.
- Liu F, Huang H, Xu ZL, Qian XJ and Qiu WY** (2012) Germ cell removal after induction of cryptorchidism in adult rats. *Tissue Cell* **44**, 281–7.
- Liu Z, Chen P, Gao H, Gu Y, Yang J, Peng H, Xu X, Wang H, Yang M, Liu X, Fan L, Chen S, Zhou J, Sun Y, Ruan K, Cheng S, Komatsu M, White E, Li L, Ji H, Finley D and Hu R** (2014) Ubiquitylation of autophagy receptor optineurin by HACE1 activates selective autophagy for tumor suppression. *Cancer Cell* **26**, 106–20.
- Lue YH, Hikim AP, Swerdloff RS, Im P, Taing KS, Bui T, Leung A and Wang C** (1999) Single exposure to heat induces stage-specific germ cell apoptosis in rats: role of intratesticular testosterone on stage specificity. *Endocrinology* **140**, 1709–17.
- Maiuri MC, Zalckvar E, Kimchi A and Kroemer G** (2007) Self-eating and self-killing: crosstalk between autophagy and apoptosis. *Nat Rev Mol Cell Biol* **8**, 741–52.
- Nakatogawa H, Suzuki K, Kamada Y and Ohsumi Y** (2009) Dynamics and diversity in autophagy mechanisms: lessons from yeast. *Nature Rev Mol Cell Biol* **10**, 458–67.
- Nantel F, Monaco L, Foulkes NS, Masquillier D, LeMeur M, Henriksen K, Dierich A, Parvinen M and Sassone-Corsi P** (1996) Spermiogenesis deficiency and germ-cell apoptosis in CREM-mutant mice. *Nature* **380**, 159–62.
- Ogi S, Tanji N, Yokoyama M, Takeuchi M and Terada N** (1998) Involvement of Fas in the apoptosis of mouse germ cells induced by experimental cryptorchidism. *Urol Res* **26**, 17–21.
- Ohsumi Y** (2014) Historical landmarks of autophagy research. *Cell Res* **24**, 9–23.
- Oltvai ZN, Milliman CL and Korsmeyer SJ** (1993) Bcl-2 heterodimerizes in vivo with a conserved homolog, Bax, that accelerates programmed cell death. *Cell* **74**, 609–19.
- Peterson JS, Timmons AK, Mondragon AA and McCall K** (2015) The end of the beginning: cell death in the germline. *Curr Topics Dev Biol* **114**, 93–119.

- Pettersson A, Richiardi L, Nordenskjold A, Kaijser M and Akre O** (2007) Age at surgery for undescended testis and risk of testicular cancer. *New Engl J Med* **356**, 1835–41.
- Schulz RW and Miura T** (2002) Spermatogenesis and its endocrine regulation. *Fish Physiol Biochem* **26**, 43–56.
- Sharlip ID, Jarow JP, Belker AM, Lipshultz LI, Sigman M, Thomas AJ, Schlegel PN, Howards SS, Nehra A, Damewood MD, Overstreet JW and Sadovsky R** (2002) Best practice policies for male infertility. *Fertil Steril* **77**, 873–82.
- Shikone T, Billig H and Hsueh AJ** (1994) Experimentally induced cryptorchidism increases apoptosis in rat testis. *Biol Reprod* **51**, 865–72.
- Song BS, Yoon SB, Kim JS, Sim BW, Kim YH, Cha JJ, Choi SA, Min HK, Lee Y, Huh JW, Lee SR, Kim SH, Koo DB, Choo YK, Kim HM, Kim SU and Chang KT** (2012) Induction of autophagy promotes preattachment development of bovine embryos by reducing endoplasmic reticulum stress. *Biol Reprod* **87**, 8, 1–11.
- Xi M, Cheng L, Wan YP and Hua W** (2015) [Incidence of depression and its related factors in cryptorchidism patients after surgical treatment]. *Zhonghua nan ke xue [in Chinese]* **21**, 57–60.
- Xu YR, Dong HS and Yang WX** (2016) Regulators in the apoptotic pathway during spermatogenesis: killers or guards? *Gene* **582**, 97–111.
- Yang E, Zha J, Jockel J, Boise LH, Thompson CB and Korsmeyer SJ** (1995) Bad, a heterodimeric partner for Bcl-XL and Bcl-2, displaces Bax and promotes cell death. *Cell* **80**, 285–91.
- Yin Y, DeWolf WC and Morgentaler A** (1998) Experimental cryptorchidism induces testicular germ cell apoptosis by p53-dependent and-independent pathways in mice. *Biol Reprod* **58**, 492–6.
- Yin Y, Hawkins KL, DeWolf WC and Morgentaler A** (1997) Heat stress causes testicular germ cell apoptosis in adult mice. *J Androl* **18**, 159–65.
- Zhang MQ, Jiang M, Bi Y, Zhu H, Zhou ZM and Sha JH.** (2012) Autophagy and apoptosis act as partners to induce germ cell death after heat stress in mice. *PLoS One* **7**, e41412.